

HORIZONTAL AXIS WIND TURBINE FLOW FIELD ANALYSIS AND PROSPECTS FOR PERFORMANCE ENHANCEMENT*

Andreea BOBONEA¹, Corneliu BERBENTE², Mihai Leonida NICULESCU³

The wind energy is deemed as one of the most durable energetic variants of the future because the wind resources are immense. Therefore research in this field must be continuous and interdisciplinary. The objective of these investigations is to improve the wind turbines aerodynamic performance and increase their operational range by inducing complete or partial flow reattachment. One of the main methods used in active flow control is the usage of blowing devices with constant jet. Through steady CFD simulations for an horizontal axis wind turbine, this study is trying to analyse the flow field around the wind turbine and also to highlight the impact of constant blowing at the leading edge of each blade in enhancing the wind turbine performance.

Keywords: Horizontal Axis Wind Turbine, Active Flow Control, Blowing Jet, CFD.

1. Introduction

Wind energy has steadily established itself as one of the most reliable and affordable renewable energy resources. Wind turbine design has to be improved continually, i.e. basic research in aerodynamics, structural dynamics, dynamic forces, new materials, feasibility studies into new systems, determination of noise and its reduction methods, optimization methods.

Current efforts focus on increasing their aerodynamic efficiency and operational range through active flow control with the help of blowing devices with constant or pulsed jets. By adding high-stored momentum air through slots into the boundary layer, they overcome adverse pressure gradients and postpone

¹ Ph. D. Student, Aerospace Engineering Faculty, University POLITEHNICA of Bucharest, Romania, e-mail: andreea_911@yahoo.com

² Professor, Aerospace Engineering Faculty, University POLITEHNICA of Bucharest, Romania, e-mail: berbente@yahoo.com

³ Scientific Researcher, National Institute for Aerospace Research "Elie Carafoli" - INCAS, Bucharest, Romania, e-mail: mniculescu@incas.ro

*The results presented in this article were obtained with the support of Ministry of Labour, Family and Social Protection through Sectorial Operational Programme Human Resources Development 2007-2013, Contract no. POSDRU/107/1.5/S/76813.

separation. Pulsed blowing sends short pulses rather than a continuous jet of fluid into the boundary layer and has been found to be more effective. Experimental investigations [1-5] and 2D numerical simulations [6, 7] of active manipulation of separated flows over airfoils has been the focus of a number of investigations for many years.

2. Blade Design Tool

The turbine studied in this paper is a 1.5 MW horizontal-axis wind turbine used to extract the energy from the wind with little environmental impact, by converting the kinetic energy of the wind directly to mechanical power. The turbine has been dimensioned using the blade element momentum method implemented into MathCAD. For this method we used as design input:

- the speed of the current, $V_\infty = 10$ m/s;
- the tip speed ratio, $\lambda = 7$;
- the number of blades, $B = 3$;
- the estimated power coefficient, lower than the Betz limit, $c_p = 0.468 < 0.593$;
- the power desired to be obtained, $P = 1.5$ MW.

Chosen airfoils used for the blade design are four extensively used nowadays profiles, S809, S810, S814 and S815 developed by NREL for horizontal axis wind turbine. The lift and drag coefficients for these profiles have been computed, for different angles of attack, using the XFOIL tool. The distribution of each profile along the radius was set using the design recommendations [8].

Table 1.

Design Parameters for chosen airfoils

Airfoil	r/R	Re.No. (x10 ⁶)	t/c	C _{lmax}	C _{dmin}	C _{mo}
S810	0.95	2.0	0.180	0.90	0.006	-0.05
S809	0.75	2.0	0.210	1.00	0.007	-0.05
S814	0.40	1.5	0.240	1.30	0.012	-0.15
S815	0.30	1.2	0.260	1.10	0.014	-0.15

If there were no structural requirements, this is how a wind turbine blade would be proportioned, but of course the blade needs to support the lift, drag and gravitational forces acting on it. These structural requirements generally mean the airfoil needs to be thicker than the aerodynamic optimum, especially at locations towards the root (where the blade attaches to the hub) where the bending forces are bigger.

The angle of attack at the design point is set to vary from 9° at the tip of the blade to 12° at the root of the blade as recommended in Dumitrescu et al. [9]. The sizing of the rotor resulted in a diameter of 41.5 m which was determined using the kinetic turbine power equation:

$$D = \left(P \cdot \left(\frac{\pi}{4} \cdot c_p \cdot \frac{\rho}{2} \cdot V_\infty^3 \right)^{-1} \right)^{0.5} \quad (1)$$

The second method involves nonlinear equations solved at all considered radii with the complication of multiple solutions. The first method is robust and was adopted for the tool, implemented in MathCAD. Variable aerodynamic coefficients are used, instead of single values. Lift and drag versus angle of attack are least square interpolated in order to provide clean and easy to use input. Experimental or numerical values are used, depending on the availability. XFOIL predicted results are typically used, when there are no wind tunnel results, or Reynolds number is not properly matched.

The discrete chord distribution is least-square reconstructed and modified at the root, taking into account the hub radius. The modification consists in replacing some part of the root curve with a polynomial one, maintaining continuity of the first order derivative. This connection curve is quite steep, because the available hub has a small inner radius for the root of the blade. The airfoil is correspondingly modified in the connection zone, using a nonlinear weighted lofting between the root circular section and the ideal blade. Solidity coefficient is not directly imposed, but it can be influenced by adjusting the local angle of attack of the blade element.

The output of the design method [10] consisted of:

- power coefficient curve as a function of tip speed ratio;
- chord distribution along the radius, Fig.1.;
- twist angle distribution along the radius, Fig. 2.;

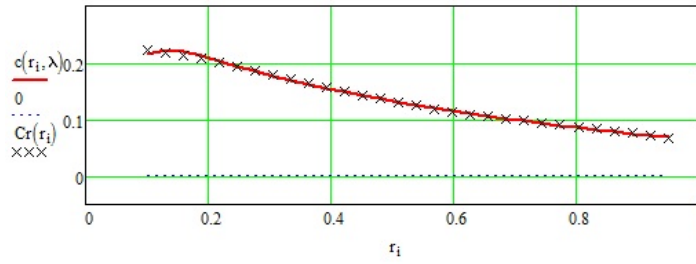


Fig. 1. Chord distribution along the radius for 1.5MW HAWT

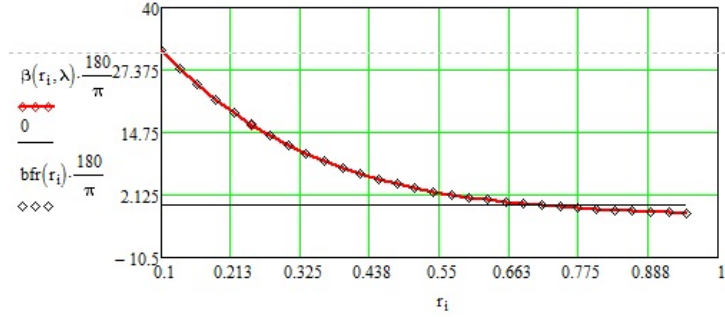


Fig. 2. Twist angle distribution for 1.5MW HAWT.

The blade geometry shown in Fig. 3 was generated in CATIA V5 using a CATScript macro language. The polynomial functions of the chord and twist angle distributions, as well as the ones of the S810, S809, S814 and S815 profiles, were implemented as parametric curve elements, while the leading and trailing edge curves were introduced as combination of their analytical defined projections. After the initial design has been generated, the shape of the blade is optimized to better meet the structural requirements.

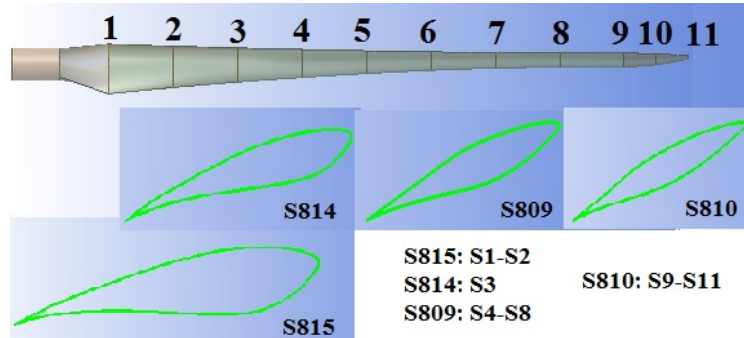


Fig. 3. Blade geometry and the profile distribution along the radius

To increase thickness near the root without creating a very short, fat, airfoil section, some designs use a “flatback” section. This is either a standard section thickened up to a square trailing (back) edge, or a longer airfoil shape that has been truncated. This reduces the drag compared to a rounder section, but can generate more noise so its suitability depends on the wind farm site.

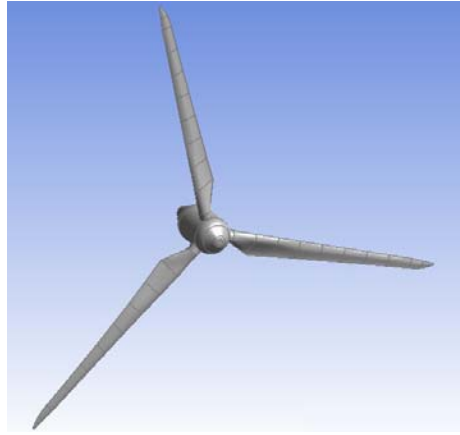


Fig. 4 Rotor geometry, front view

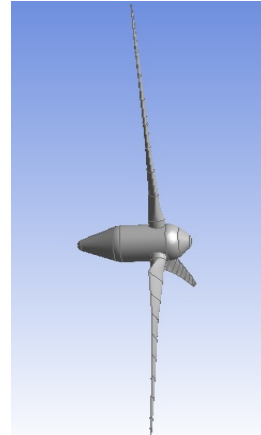


Fig. 5. Rotor geometry, side view

3. Numerical Simulation

The 3D numerical modeling of the viscous flow has been performed with the CFD commercial code FLUENT [11]. The flow was assumed incompressible and fully turbulent. The shear-stress transport (SST) $k-\omega$ turbulence model developed by Menter [12] was used in order to combine the advantages of the robust and accurate formulation of the Wilcox $k-\omega$ model [13] in the near-wall region with the free-stream independence of the $k-\epsilon$ model in the far field.

The simulations have been carried out using the finite volume method [14,15] of the incompressible Reynolds averaged Navier-Stokes equations (RANS) [14, 16].

The mesh was generated in NUMECA's HEXPRESS tool, using hexahedral volume elements and consists of two domains, one considered stationary having approximately 1 million cells and another housing the turbine rotor having approximately 20 million cells.

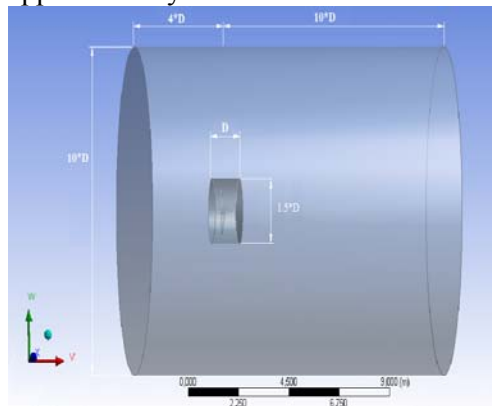


Fig. 6. Computational domain

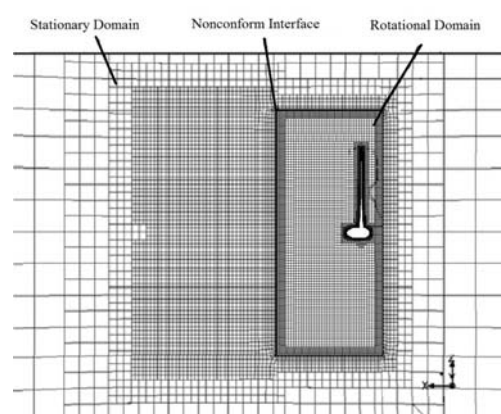


Fig. 7. Meshing detail

An O type grid was used around the wind turbines walls. The first boundary layer height of $ds=0.000015\text{m}$ so as to be able to obtain the dimensionless wall distance $y^+=1$, with the height growing factor of 1.1.

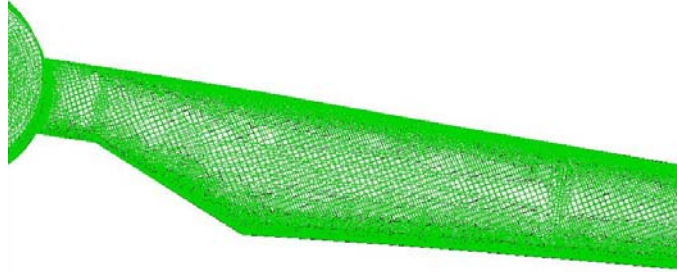


Fig.8. The surface mesh on a blade

In the present study, the first simulations were performed on the designed horizontal axis wind turbine, for investigation of the flow field around the wind turbine. All later tests were performed with the constant-blowing actuation defined at the trailing edge as velocity inlet, with a standard incompressible jet. The jet velocity parameter $U_{jet}=4.42\text{m/s}$, was extracted from the following formula:

$$C_\mu = \frac{\rho_{jet} \cdot U_{jet}^2 \cdot A_{jet}}{\frac{1}{2} \rho_\infty \cdot U_{ref}^2 \cdot A_{ref}} \quad (2)$$

where $A_{ref} = \pi r^2$, blowing momentum coefficient, $C_\mu=0.5\%$, reference velocity $U_{ref}=V_\infty=10\text{m/s}$.

4. Results

An evaluation of the turbine performance enhancement was made by monitoring the torque used to determine the power of the turbine, respectively the power coefficient for reference configuration and for active flow control control configuration. From Fig.9, it can be seen a significant increase (almost 7%) of the momentum coefficient with the help of active flow control, thus resulting a power coefficient of 0.43.

$$P = M \cdot \omega \Rightarrow c_p = c_M \cdot \lambda \quad (3)$$

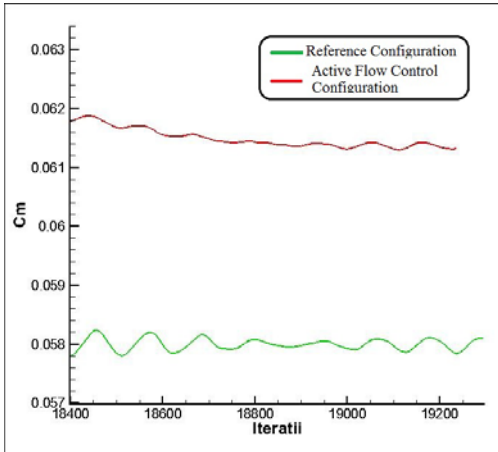


Fig. 9. Momentum coefficient comparison

The turbulent viscosity ratio for a meridional section is presented in Fig.10. and Fig.11. It can be observed a small decrease of the turbulent viscosity ratio in the case of the configuration with the active flow control.

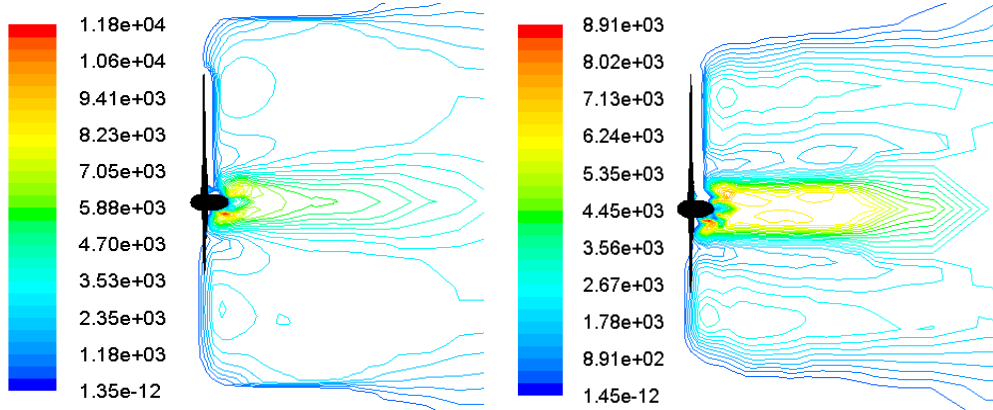


Fig. 10. Turbulent viscosity ratio without AFC

Fig. 11. Turbulent viscosity ratio with AFC

The plots displayed from Fig. 12 to Fig. 17 show the corresponding numerical result of the surface streamlines for three cylinder sections placed at $r=10\text{m}$, $r=20\text{m}$, $r=30\text{m}$. On the suction side of the blade, flow separation becomes visible by the direction of surface streamlines (see Fig. 12, Fig. 14 and Fig. 16). By inducing a velocity jet at the trailing edge, the boundary layer separation is delayed (Fig. 15, Fig. 17) or the flow is nicely attached to the profile (Fig. 13).

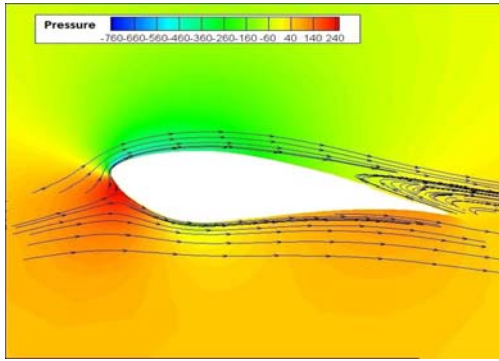


Fig. 12. Relative flow streamlines and relative static pressure distributions for a cylindrical section at $r=10m$, Reference Configuration

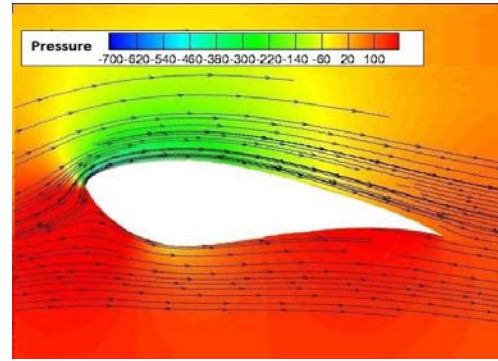


Fig. 13. Relative flow streamlines and relative static pressure distributions for a cylindrical section at $r=10m$, Active Flow Control Configuration

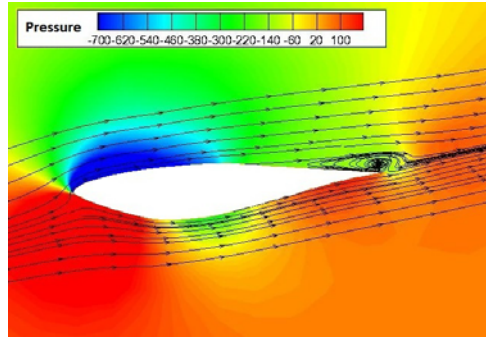


Fig. 14. Relative flow streamlines and relative static pressure distributions for a cylindrical section at $r=20m$, Reference Configuration

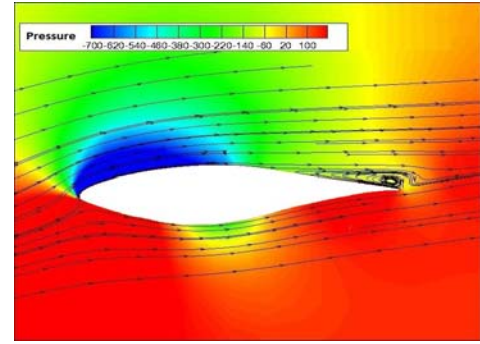


Fig. 15. Relative flow streamlines and relative static pressure distributions for a cylindrical section at $r=20m$, Active Flow Control Configuration

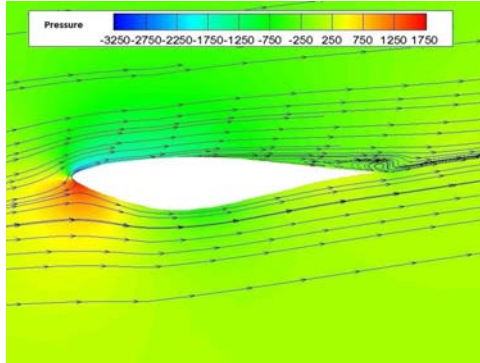


Fig. 16. Relative flow streamlines and relative static pressure distributions for a cylindrical section at $r=30m$, Reference Configuration

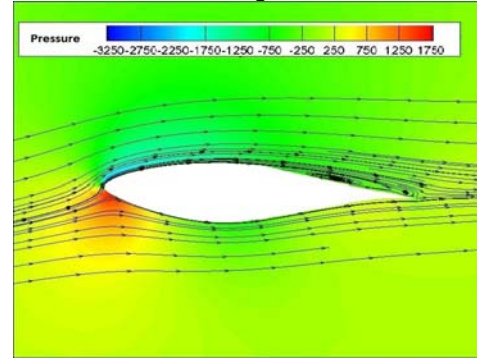


Fig. 17. Relative flow streamlines and relative static pressure distributions for a cylindrical section at $r=30m$, Active Flow Control Configuration

5. Conclusions

In the present study, a number of RANS simulations were performed on a specially designed wind turbine blade. The design procedure was proved to generate accurate blade geometry parameters. The numerical analysis was found to be useful for determining the peak efficiency of the turbine. The computed performance curve was found to present a deviation of 17% from the ideal designed performance curve.

The simulations based on finite volume method were performed to characterize in detail the three-dimensional behavior of the flow in order to identify the recirculation zones, which the classical methods of design, like blade element momentum theory cannot predict. This information is very useful in the rotor's geometry optimization and the active flow control applied to increase the wind turbine performance.

Up to now, all simulations for the active flow configuration were done for a single velocity jet, and it is known that the variation of this parameter is important in achieving the optimum performance for a configuration. Further work will be dedicated to optimize the rotor's geometry and the active flow control applied to improve the wind turbine performance.

R E F E R E N C E S

- [1] *J.R.Zayas,C.P.van Dam, R. Chow, J.P.Baker, E.A.Mayda*, Active Aerodynamic Load Control for Wind Turbine Blades, Wind Energy Technology Division, Sandia National Laboratories
- [2] *O. Stalnov, A. Kribus, A. Seifert*, Evaluation of active flow control applied to wind turbine blade section, Journal of Renewable and Sustainable Energy 2, 2010
- [3] *R.C. Nelson, T.C. Corke, H. Othman*, A Smart Wind Turbine Blade Using Distributed Plasma Actuators for Improved Performance, 46th Aerospace Sciences Meeting, January 7-10, 2008, Reno, Nevada
- [4] *O. Eisele, G. Pechlivanoglou, C.N. Nayeri, C.O. Paschereit*, Flow Control Using Plasma Actuators at The Root Region of Wind Turbine Blades, Institut für Strömungsmechanik und Technische Akustik, TU Berlin
- [5] *S.J. Johnson, C.P.van Dam, D.E. Berg*, Active Load Control Techniques for Wind Turbines, Sandia Report, SAND2008-4809
- [6] *A. Bobonea*, Impact of Pulsed Blowing Jet on Aerodynamic Characteristics of Wind Turbine Airfoils, 9th International Conference on Mathematical Problems in Engineering, Aerospace and Sciences, Vienna, Austria, published in: American Institute of Physics, 2012.
- [7] *A. Bobonea*, Unsteady Computational Simulation for Active Aerodynamic Control of a Horizontal Axis Wind Turbine, 10th International Conference on Numerical Analysis and Applied Mathematics, Kos, Greece, published in: American Institute of Physics, 2012.
- [8] *T. Burton, N. Jenkins, D. Sharpe, E. Bossanyi*, Wind Turbine Blade Aerodynamics, WindEnergy Handbook 2, ISBN 0470699752 (2011).
- [9] *H. Dumitrescu, A. Georgescu*, Calculul elicei, published by House of Romanian Academy, Bucharest, 1990, pp 250-290.

- [10] *A. Bobonea, M. V. Pricop*, Design of Horizontal-Axis Wind Turbine Using Blade Element Momentum Method, 11th International Conference on Numerical Analysis and Applied Mathematics, Rhodos, Greece, published in: American Institute of Physics, 2013.
- [11] ANSYS FLUENT Theory Guide, Release 14.0, November 2011.
- [12] *F.R. Menter*, Two Equation Eddy-Viscosity Turbulence Models for Engineering Applications, AIAA Journal, Vol. 32, No. 8, pp. 1598-1605, August 1994.
- [13] *D. C. Wilcox*, Comparison of two-equation turbulence models for boundary layers with pressure gradient, AIAA Journal, Vol. 31, No. 8, pp. 1414-1421, 1993
- [14] *S. Dănilă, C. Berbente*, Metode numerice în dinamica fluidelor, Editura Academiei Romane, Bucuresti, 2003.
- [15] *C. Hirsch*, Numerical Computation of Internal and External Flow, Volume 1: The Fundamentals of Computational Fluid Dynamics, Elsevier, Second Edition, 2007.
- [16] *C. Hirsch*, Numerical Computation of Internal and External Flow, Volume 2: Computational Methods for Inviscid and Viscous Flows, John Wiley and Sons, New York, 1990.